Detection of human T lymphotropic virus type-I bZIP factor and tax in the salivary glands of Sjögren's syndrome patients

H. Nakamura[1], H. Hasegawa[2], D. Sasaki[2], A. Takatani[1], T. Shimizu[1], S. Kurushima[1], Y. Horai[3], Y. Nakashima[4], T. Nakamura[5], J. Fukuoka[6], A. Kawakami[1]

[1]Department of Immunology and Rheumatology, Unit of Advanced Medical Sciences, Division of Advanced Preventive Medical Sciences, Nagasaki University Graduate School of Biomedical Sciences; [2]Department of Laboratory Medicine, Nagasaki University Hospital; [3]Clinical Research Centre, National Hospital Organization Nagasaki Medical Centre; [4]Department of Immunology and Rheumatology, Sasebo City General Hospital; [5]Department of Social Work, Faculty of Human and Social Studies, Nagasaki International University; [6]Department of Pathology, Nagasaki University Hospital, Nagasaki, Japan.

Hideki Nakamura, MD, PhD
Hiroo Hasegawa, MD, PhD
Daisuke Sasaki, PhD
Ayuko Takatani, MD
Toshimasa Shimizu, MD
Shota Kurushima, MD
Yoshiro Horai, MD, PhD
Yoshikazu Nakashima, MD, PhD
Tatsufumi Nakamura, MD, PhD
Junya Fukuoka, MD, PhD
Atsushi Kawakami, MD, PhD

Please address correspondence to:
Dr Hideki Nakamura,
Department of Immunology and Rheumatology, Unit of Advanced Medical Sciences, Division of Advanced Preventive Medical Sciences, Nagasaki University Graduate School of Biomedical Sciences, 1-7-1 Sakamoto, Nagasaki City, 852-8501 Nagasaki, Japan.
E-mail: nhideki@nagasaki-u.ac.jp

Received on December 7, 2017; accepted in revised form on February 12, 2018.

Clin Exp Rheumatol 2018; 36 (Suppl. 112): S51-S60.

Key words: Sjögren's syndrome, HBZ, tax, HTLV-I

Funding: this work was supported in part by JSPS KAKENHI grant no. JP16K09899.
Competing interests: none declared.

ABSTRACT

Objective. *To detect HTLV-I bZIP factor (HBZ), tax and relevant molecules in labial salivary glands (LSGs) from patients with Sjögren's syndrome (SS).*

Methods. *The expressions of HBZ and tax in T cell lines and LSGs were analysed by in situ hybridisation (ISH) or real time PCR. The expressions of forkhead box P3 (Foxp3) and p65 in immunohistochemistry were quantified.*

Results. *After specificity of ISH probes was determined in 5 T cell lines, in LSGs from an adult T-cell leukaemia (ATL) patient and 3 HTLV-I-associated myelopathy (HAM)-SS patients, both HBZ and tax signals were detected in infiltrating mononuclear cells (MNCs) and ducts, and HBZ and tax were dominantly expressed in MNCs of ATL and HAM-SS, respectively. HBZ was dominantly observed in LSGs from 8 HTLV-I asymptomatic carrier (AC)-SS patients; faint expression of HBZ was observed in LSGs from 5 HTLV-I-seronegative SS patients. No cell adhesion molecule 1(CADM1) expressed in LSGs from the ATL patient. Although Foxp3 expression was observed in LSG MNCs of all of the SS patients, the ATL patient's expression was significantly greater than that of the AC-SS ($p<0.01$) and HTLV-I-seronegative SS ($p<0.01$) patients. The Foxp3 expression was similar in ATL and HAMSS, but significantly higher in HAM-SS than AC-SS ($p<0.05$). p65 was expressed in LSG MNC nuclei from all SS patients and co-expressed with Foxp3. The expressions of Foxp3 in ducts differed according to HTLV-I infection.*

Conclusion. *These results suggest that HBZ-mediated Foxp3 expression is partly associated with the pathogenesis of HTLV-I-seropositive SS.*

Introduction

An association has been reported between human T lymphotropic virus type I (HTLV-I) and Sjögren's syndrome (SS), an autoimmune disease characterised by xerostomia, xerophthalmia and the presence of autoantibodies including anti-Ro/SS-A and La/SS-B antibodies (1-3). Although the causative factors of SS remains clarified, elucidation of pathogenesis of SS is of great interest in view of treatment strategy (4). In our previous experiments, we demonstrated both an epidemiological relationship between HTLV-I and SS, and a high prevalence of SS among patients with HTLV-I-associated myelopathy (HAM) (5). We also obtained some findings including less salivary gland destruction and low frequency of germinal centre formation in HTLV-I-seropositive SS (6-8). Our recent study also demonstrated low frequencies of anti-Ro/SS-A antibody and antinuclear antibody in patients with HAM-SS (9). Other research groups (10, 11) also reported that they detected HTLV-I *tax* signals or related molecules in the labial salivary glands (LSGs) of SS patients, following Shattles *et al*. 1992 report describing the presence of endogenous retrovirus in LSGs of patients with SS (12). These previous findings suggested direct association between SS and retroviruses.

Because salivary glands of an HTLV-I *tax* transgenic mouse model showed Tax protein expression (13), *tax* is thought to be associated with the induction of inflammation in HTLV-I-seropositive SS. The aetiology of HTLV-I-seropositive SS has focused mainly on the presence of the *tax* gene in LSGs, but the importance of HTLV-I bZIP factor (*HBZ*) - which is derived from the minus strand of the HTLV-I gene - in the pathogenesis of adult T-cell leukaemia (ATL) and HAM has been demonstrated (14). Because *HBZ* has the potential to cause inflammation as well as carcinogenicity in ATL (15), the relationship between *HBZ* and *tax* should be estab-

lished in HTLV-I-associated diseases.
In addition, the phenotype of HTLV-I infected lymphocytes in ATL is $CD4^+CD25^+Foxp3^+$ regulatory T cells (Tregs) (16), and the involvement of $Foxp3^+$ T cells in HTLV-I-infected LSGs is thought to be important in HTLV-I-associated SS. The present report is the first to describe the *HBZ*/*tax* and Foxp3 expression and distribution in LSGs from patients with HTLV-I-seropositive and seronegative SS. Although the vast majority of patients with SS have no HTLV-I infection, the findings in this study may help to clarify the relationship between HTLV-I and SS in areas in which SS is endemic.

Materials and methods

Patients

We analysed 11 HTLV-I-seropositive patients with SS (3 patients with HAM-SS and 8 HTLV-I asymptomatic carrier [AC] SS patients), 5 HTLV-I-seronegative SS patients, and 3 normal subjects. The classification of SS was conducted using the American-European Consensus Group (AECG) classification criteria (17). All SS patients showed a positive result on a salivary gland biopsy with at least one focus that consisted of >50 lymphocytes per 4 mm^2. Normal subjects had been examined after reporting dry mouth and eye symptoms, and had been categorised as non-SS according to the AECG classification criteria after having been examined based on their report of dry mouth and eye symptoms. The diagnostic criteria for HAM (18) issued by the Ministry of Health, Labour and Welfare of Japan were used. Anti-HTLV-I antibody in the serum and cerebral spinal fluid of the HAM patients was positive.
To screen for anti-HTLV-I antibodies, a chemiluminescent enzyme immunoassay (normal range: 1.0 cutoff index; Fujirebio, Tokyo) was employed. Salivary glands from a patient with ATL were used as a positive control for HTLV-I infection. The diagnosis of ATL was confirmed based on the presence of atypical lymphocytes in peripheral blood, positive anti-HTLV-I antibody, elevated soluble interleukin-2 receptor, and the presence of infiltrating cells in salivary glands that showed CD3/CD4 positive T cells with irregularity, as described previously (19). Southern blot analysis of peripheral blood in a patient with ATL showed HTLV-I provirus clonality with a monoclonal band processed by EcoRI. HTLV-I proviral load (PVL) in peripheral blood in a patient with ATL was 25% as determined by quantitative polymerase chain reaction at the Department of Laboratory Medicine of Nagasaki University Hospital. Because these cells in LSGs showed difference in size with nuclear constriction with T cell dominance and the markers UCHL1, CD3 and CD4 rather than B cell markers including L26 and CD79a, these findings show a mixture of chronic inflammation and direct infiltration of ATL cells into LSGs. The decreased saliva secretion and xerostomia with massive infiltration of $CD3^+CD4^+$ T lymphocytes in our ATL patient resembled SS, because the patient met three of the AECG criteria (17) for SS classification.

Antibodies and reagents

Mouse anti-Foxp3 antibody was obtained from eBiosciences (San Diego, CA). Rabbit anti-cytokeratin 8/18 antibody was purchased from Dako, Agilent Pathology Solutions (Santa Clara, CA). Rabbit-SYNCAM/CADM1 antibody was purchased from RayBiotech, Inc (Norcross, GA). Rabbit anti-NF-κB p65 antibody was purchased from Santa Cruz Biotechnology, (Santa Cruz, CA). The Histofine® Simple Stain MAX-PO™ (M) kit, MAX-PO® (R) kit, Alkaline Phosphatase:AP® (R) kit and Fast Red II substrate kit were purchased from Nichirei Biosciences (Tokyo). The 3.3'-diaminobenzidine was purchased from Dojindo (Kumamoto, Japan).

Cell lines

Jurkat and MOLT-4 were used as HTLV-I uninfected cell lines. HCT-5 (3) that was established from cerebrospinal fluid from a patient with HAM and two cell lines EE8 and YK8 from patients with smoldering ATL (20) were employed.

LSG biopsy

We performed an LSG biopsy from the lower lip of each patient and control subject after administering local anesthesia. All SS patients were classified according to the AECG classification criteria. Informed consent for the use of samples obtained by the biopsy was obtained in writing from all of the participants.
The study was conducted with the approval of the Ethics Committee (Human Studies) of Nagasaki University Hospital (approval number 09102822-4).

Real-time PCR

Quantitative real-time PCR and primer design (*tax*: accession no. AF033817; *HBZ*: accession no. AB219938) were carried out at Hokkaido System Science Co., Ltd. Three Primers sets for *tax* are shown as follows; first forward primer: 5'- CTACCCGAGGACTGTTTGCCCACC -3', first reverse primer: 5'- GTTGAGTGGAACGGAAGGAGGCCG -3', second forward primer: 5'- TCTACCCGAGGACTGTTTGCCCACC -3', second reverse primer: 5'- GTTGAGTGGAACGGAAGGAGGCCG -3', third forward primer: 5'- CGCCTACATCGTCACGCCCTACTG -3'. Three Primers sets for HBZ are shown as follows; first forward primer: 5'- GAGGAGAAGGCACGGCGCAGGAG -3', first reverse primer: 5'- CCTTGTCTCCACTTGCGCTCACGG -3', second forward primer: 5'- CAGAACGCGACTCAACCGGCGTG -3', second reverse primer: 5'- CCGTCCACCAATTCCTCCACCAGC -3', third forward primer: 5'- GTCCTTGGAGGCTGAACGGAGGAAG -3', third reverse primer: 5'- TTATTGCAACCACATCGCCTCCAGC -3'. After RNA extraction with an RNeasy Mini Kit (QIAGEN, Venlo, Netherlands), complementary (c) DNA adjustment and determination of the primer concentration were performed. Real time amplification was carried out by using a QuantiFast SYBR Green PCR kit (QIAGEN). The composition of the reaction solution consisted of 7.5 μL of 2x Master Mix, 1.5μL of primer, 1.0μL of template cDNA and 5.0μL of nucleus free water. Reaction conditions were set as follows: initial denaturation at 95°C for 3 min, followed by 40 cycles of denaturation at 95°C for 10 sec, annealing and extension at 60°C for 30 sec.

The results were captured using a CFX384 Touch Real-Time PCR Detection System (BIO-RAD, Hercules, CA).

In situ hybridisation

For the *in situ* hybridisation (ISH), cell lines and the LSG sections were sent to the Tokushima Molecular Pathology Institute, and the highly sensitive reagent ViewRNA™ purchased from Affimetrix/Panomics (Santa Clara, CA) was used there to detect *HBZ* and *tax* messages. The specificity of the ViewRNA™ probe is described in the instructions provided by Affimetrix/Panomics. Briefly, the oligonucleotides in the probe contain two components; the lower component is complementary to the target RNA, and shows effects on specificity toward the target RNA molecule without amplifying the background signal. For the ISH, T cell lines and LSGs from a patient with ATL, 3 HAM patients with SS, 3 HTLV-I AC patients with SS, 3 HTLV-I-seronegative patients with SS, and the 3 normal control subjects were used.

The ISH was performed according to the manufacturer's instructions at the Tokushima Molecular Pathology Institute. The Quantigene ViewRNA® probes against *HBZ* and *tax* (HTLV *HBZ* probe: accession no. AB219938, VF6-19284; HTLV *tax* probe: accession no. AF033817, VF1-19939) were designed and manufactured by Affymetrix. Briefly, after deparaffinisation, the slides were treated with protease for 10 min at 40°C. Following endogenous alkaline phosphatase inactivation, preamplifier reaction for 25 min and amplifier reaction for 15 min were performed at 40°C. The slides were then labeled with each probe for 15 min at 40°C, followed by colour development by reaction with Fast Blue and Fast Red (alkaline phosphatase (AP) substrates). Finally, the slides were fixed in 10% formalin and mounted with aqueous mounting medium.

Immunohistochemistry

For immunohistochemistry, we used LSGs from the single patient with ATL, 3 HAM patients with SS, 8 HTLV-I AC patients with SS, 5 HTLV-I-seronegative patients with SS, and 3 normal control subjects. A tissue array (US Biomax Inc.; Rockville, MD) including 4 types of carcinoma was used for control toward cell adhesion molecule 1(CADM1). Formalin-fixed, paraffin-embedded sections (3 μm thick) from the LSGs of patients and controls were mounted on glass slides precoated with aminopropyltriethoxysilane. After microwave epitope retrieval and endogenous peroxidase inactivation, the sections were incubated with mouse anti-human cytokeratin 8/18 monoclonal antibody, rabbit anti-human SYNCAM/CADM1(synonym; tumour suppressor in lung cancer 1; TSLC1) monoclonal antibody, mouse anti-human Foxp3 primary antibody or rabbit anti-NF-κB p65 polyclonal antibody in a humid chamber for 60 min at room temperature followed by incubation with peroxidase-conjugated secondary antibodies for 30 min (Histofine Simple Stain MAX-PO (M) or (R); Nichirei Biosciences). The colour was developed by soaking the sections in DAB and H_2O_2, then counterstaining by Mayer's haematoxylin solution. For double staining, incubation with primary antibodies including mouse anti-Foxp 3 monoclonal antibody and rabbit anti-NF-κB p65 polyclonal antibody was followed by incubation with a cocktail including Histofine Simple Stain MAX-PO (M) and Histofine Simple Stain AP (R). Then, the slides were reacted with DAB solution and Fast Red II solution for colour development. For the internal control, mouse IgG1 and normal rabbit serum were used.

The images were captured by a digital microscope colour camera (DFC295; Leica Microsystems, Tokyo). A microcell count system mounted on a microscope (BZ-X700; Keyence, Osaka, Japan) was employed for quantification. Briefly, the precise DAB signal intensity was abstracted from the foci composed of MNCs after erasing all unnecessary areas. After this extraction condition was preserved, the same condition was applied to other foci to extract the DAB signal.

Statistical analysis

We used Student's *t*-test to examine the differences among the abstracted areas. For the calculation of differences among the abstracted areas, the total number of foci from all patients in each group was used. *P*-values <0.05 were accepted as significant.

Results

In situ hybridisation (ISH) and real-time PCR detection of HBZ and tax signals on cell lines

In Jurkat and MOLT-4, neither *HBZ* nor *tax* signals were detected by ISH (Fig. 1A). In contrast, a *tax* signal was detected in the large majority of HCT-5 cells, although *HBZ* was observed in more than half of tax-negative HCT-5 cells. In EE8 and YK8, a *tax* signal was detected in about half of the cells, although *HBZ* signals were detected in a smaller percentage of cells than *tax* signals (Fig. 1A). Quantitative real-time PCR revealed no *tax* signals in Jurkat and MOLT-4 cells, although HCT-5 cells showed the highest expression of *tax*, with lower expressions in YK8 and EE8 cells (Fig. 1B). The *HBZ* signal in real-time PCR was also highest in HCT cells, followed in order by YK8 and EE8, although no expression was detected in Jurkat or MOLT-4 cells (Fig. 1C).

ISH detection of HBZ and tax signals on LSGs

The *HBZ* and *tax* signals were detected by specific probes. In the LSGs from the ATL patient, many *HBZ* signals (Fig. 2A) and a few *tax* signals (Fig. 2A) were detected in MNCs. High HBZ expression was observed in thickened ducts (Fig. 2B), and some expression of *tax* was observed in all ducts (Fig. 2B). In LSGs from the HAM patients with SS, many *tax* signals and some *HBZ* signals were observed in MNCs (Fig. 2C). *HBZ* signals and *tax* signals were also detected in the ducts of LSGs from the HAM patients with SS (Fig. 2D). In LSGs from the HTLV-I AC patients with SS, a clear *HBZ* signal was detected in all ducts and infiltrating MNCs, although a low frequency of *tax* signals was observed in both ducts and MNCs (Fig. 2E). In contrast, *HBZ* expression was faintly identified in LSGs from the patients with HTLV-I-seronegative SS (Fig. 2F) and LSGs from normal subjects (Fig. 2G).

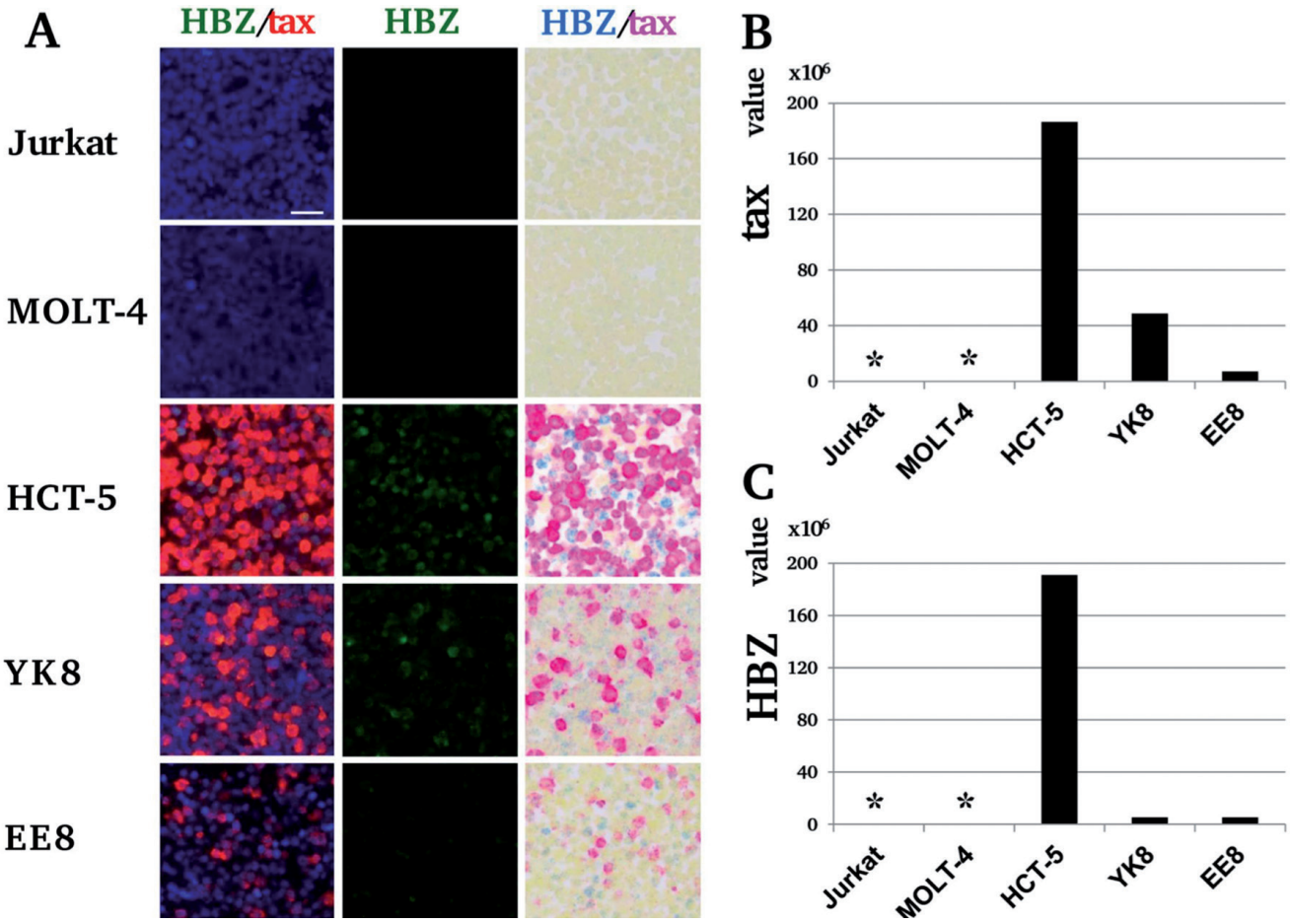

Fig. 1. Detection of *HBZ* and *tax* signals on T cell lines by ISH.
A: In Jurkat, MOLT-4, HCT-5 cells and the smoldering ATL cell lines EE8 and YK8, expression of *HBZ* and *tax* was examined by ISH using specific Quantigene ViewRNA® probes. Left and central columns show *HBZ* (green) and *tax* (red) as visualised by immunofluorescence and counter-staining with Hoechst (blue). The right column shows *HBZ* (blue) and *tax* (red) in bright field. **B**. Bar: 20 μM. B: *HBZ*. **C**: *tax* signals in cell lines were also examined by real-time PCR. **tax* and *HBZ* signals were not detected in these cells.

Expression of CADM1/TSLC1 on LSG from an ATL patient

To show the HTLV-I-induced proteins, an ATL surface marker CADM1/TSLC1 expression on LSGs was investigated. The ducts in the ATL patient were stained with cytokeratin 8/18 (Fig. 3A), a marker of epithelial cells to clearly show ducts. In LSGs from the single ATL patient, no CADM1/TSLC1 expression was found on MNCs and ducts (Fig. 3B). CADM1/TSLC1 expression was observed on adenocarcinoma tissue (Fig. 3C), although there was no expression of CADM1/TSLC1 in squamous cell carcinoma tissue (Fig. 3D). Positive CADM1/TSLC1 expression was found normal breast tissue (Fig. 3E).

Foxp3 expression in the LSGs of SS patients

In LSGs from the single ATL patient, frequent expression of Foxp3 was observed in the nuclei of infiltrating MNCs, and Foxp3 expression was also seen in the ducts (Fig. 4A). Infiltrating MNCs of LSGs from the HAM-SS patients (Fig. 4B) showed frequent nuclear expression of Foxp3. The samples from HTLV-I AC (Fig. 4C) and HTLV-I-seronegative SS patients (Fig. 4D) showed nuclear Foxp3 expression in MNCs of their LSGs, but the frequency of Foxp3 expression was less than that in the labial salivary gland MNCs from the ATL patient and the patients with HAM-SS.

No Foxp3 expression was observed in LSGs from the 3 normal controls (Fig. 4E). The ductal expression of Foxp3 was limited in the LSGs from the ATL patient (Fig. 4, insets). Our quantification of the DAB-positive area in MNCs (Fig. 4F) revealed that the LSGs from the ATL patient (no. of foci, 5; 17.2±7.7%) showed significantly larger DAB-positive areas than the LSGs from the HTLV-I AC-SS patients (n=8; no. of foci, 32; 5.1±5.3%) and HTLV-I-seronegative SS patients (n=5; no. of foci, 28; 4.4±3.3%) ($p<0.01$).

There was no significant difference in DAB-positive areas between the ATL patient and the HAM-SS patients (n=3; no. of foci, 910.4±9.4%), although the expression in the HAM-SS groups was significantly higher than that of the AC-SS group ($p<0.05$).

Expression of p65 in the LSGs of SS patients

In LSGs from the single ATL patient, the expression of p65 was frequently observed in the nuclei of infiltrating MNCs, and p65 expression was also detected in ducts (Fig. 5A). Infiltrat-

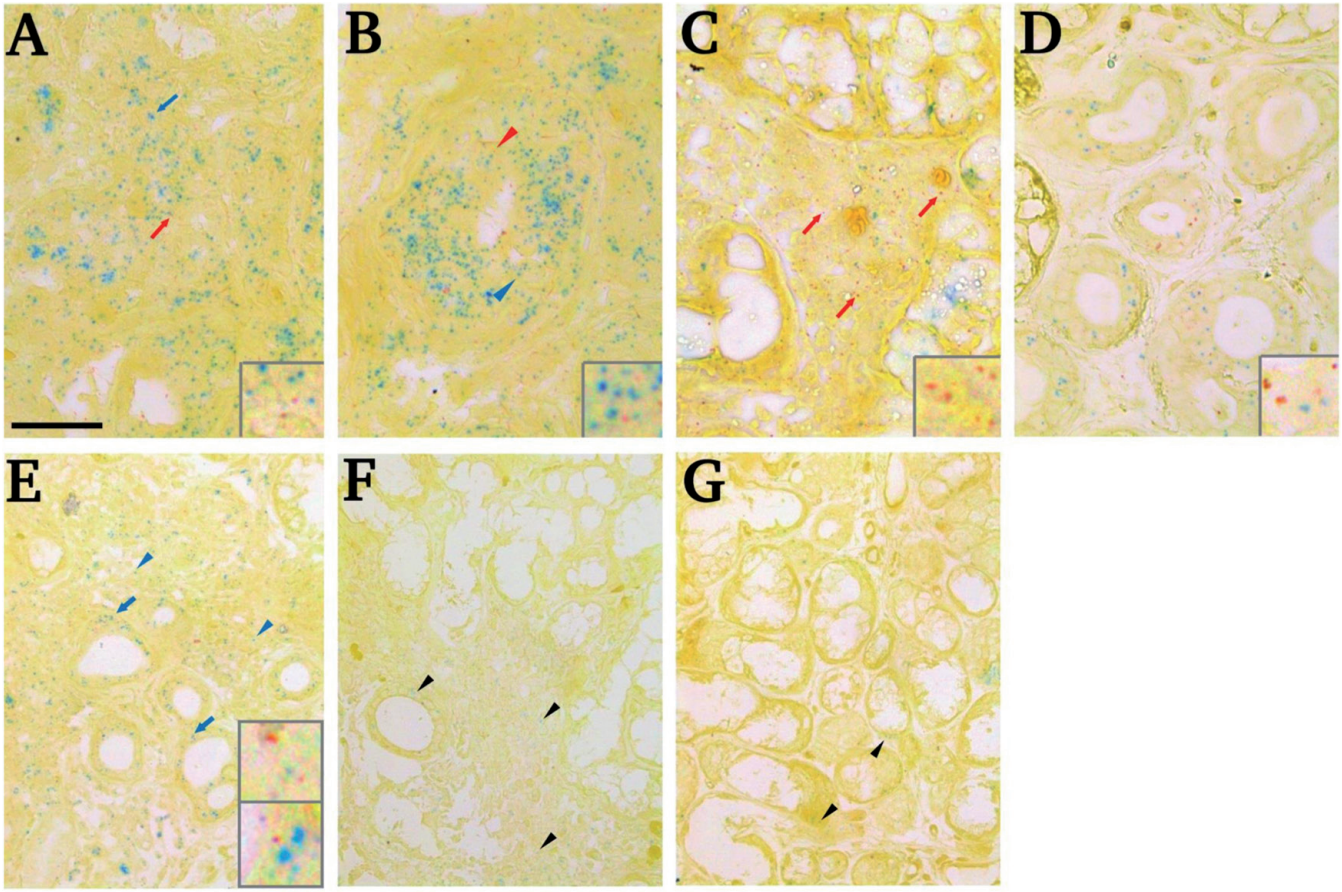

Fig. 2. Detection of *HBZ* and *tax* signals by ISH.
ISH was performed to detect *HBZ* and *tax* signals by specific Quantigene ViewRNA® probes. **A**: *HBZ* (blue arrow) and *tax* (red arrow) were observed in infiltrating MSCs from the ATL patient. **B**: *HBZ* (blue arrowhead) and *tax* (red arrowhead) were observed in ducts from the ATL patient. In LSGs from a HAM patient with SS, (**C**) *HBZ* (blue) and *tax* (red) signals in MNCs are shown. *tax*: red arrows **D**: *HBZ* (blue) and *tax* (red) signal in ducts. *HBZ* and *tax* expression in LSGs from HTLV-I AC patients with SS (**E**), HTLV-I-seronegative SS patients (**F**), and normal control (**G**). Insets show an enlarged representative signal of *HBZ* (blue) and *tax* (red). The blue arrowheads and blue arrows in panel E show *HBZ* in MNCs and ducts, respectively. *HBZ* (blue) and *tax* (red) signals in MNCs and ducts are shown in the upper inset and lower inset of panel E, respectively. The black arrowheads in panel F and G show faint *HBZ* signals. The figures show an ATL and representative data from 3 different patients. Bar: 40 μM.

ing MNCs of LSGs from the HAM-SS group (Fig. 5B) showed frequent nuclear expression of p65. The HTLV-I AC (Fig. 5C) and HTLV-I-seronegative SS patients (Fig. 5D) also showed frequent nuclear p65 expression in LSG MNCs. No p65 expression was observed in LSGs from the normal controls (Fig. 5E). The ductal expression of p65 was observed in all of the samples from the SS patients (Fig. 5 insets).

Our quantification of the size of DAB-positive areas in MNCs (Fig. 5F) revealed that there was no significant differences among LSGs from the ATL patient (no. of foci; 5: 72.0±7.4%), the HAM-SS patients (n=3, no. of foci; 9: 74.9±9.7%), the AC-SS patients (n=8, no. of foci; 32: 70.9±21.0%) and the HTLV-I-seronegative SS patients (n=5, no. of foci; 28: 73.1±11.0%), although all of the groups' percentage values were >70%.

Co-expression of p65 and Foxp3 in the LSGs of SS patients

Co-expression of the P65 and Foxp3 proteins was identified by double staining. Frequent co-expression of Foxp3 and p65 was observed in infiltrating MNCs of LSGs from the ATL patient and the HAM-SS patients (Fig. 6A, B). The HTLV-I AC (Fig. 6C) and HTLV-I-seronegative SS patients (Fig. 6D) showed frequent co-expression of nuclear Foxp3 and p65 in MNCs of their LSGs, although the frequency of co-expression was less than that of the ATL and HAM-SS patients. In LSGs from a normal control subject, cytoplasmic p65 staining of ducts was observed (Fig. 6E).

Discussion

The high expression of *HBZ* and Foxp3 in the MNCs of the LSGs from an ATL patient and HAM-SS patients compared to HTLV-I AC and HTLV-I-seronegative patients was observed in this study. In addition, frequent expression of *tax* in the MNCs was distinctive feature of HAM-SS patients.

Since most of the HTLV-I-infected cells in the LSGs of patients with SS are reported to be $CD4^+$T cells (21), the HTLV-I-induced SS pathogenesis presumably depends on HTLV-I-infected $CD4^+$T cells. The HTLV-I *tax* gene works as a trans-activator (22), which indicates that the NF-κB pathway performs a crucial role to induce pro-inflammatory cytokines. With regard to the involvement of HTLV-I infection in the LSGs of SS patients, the functions

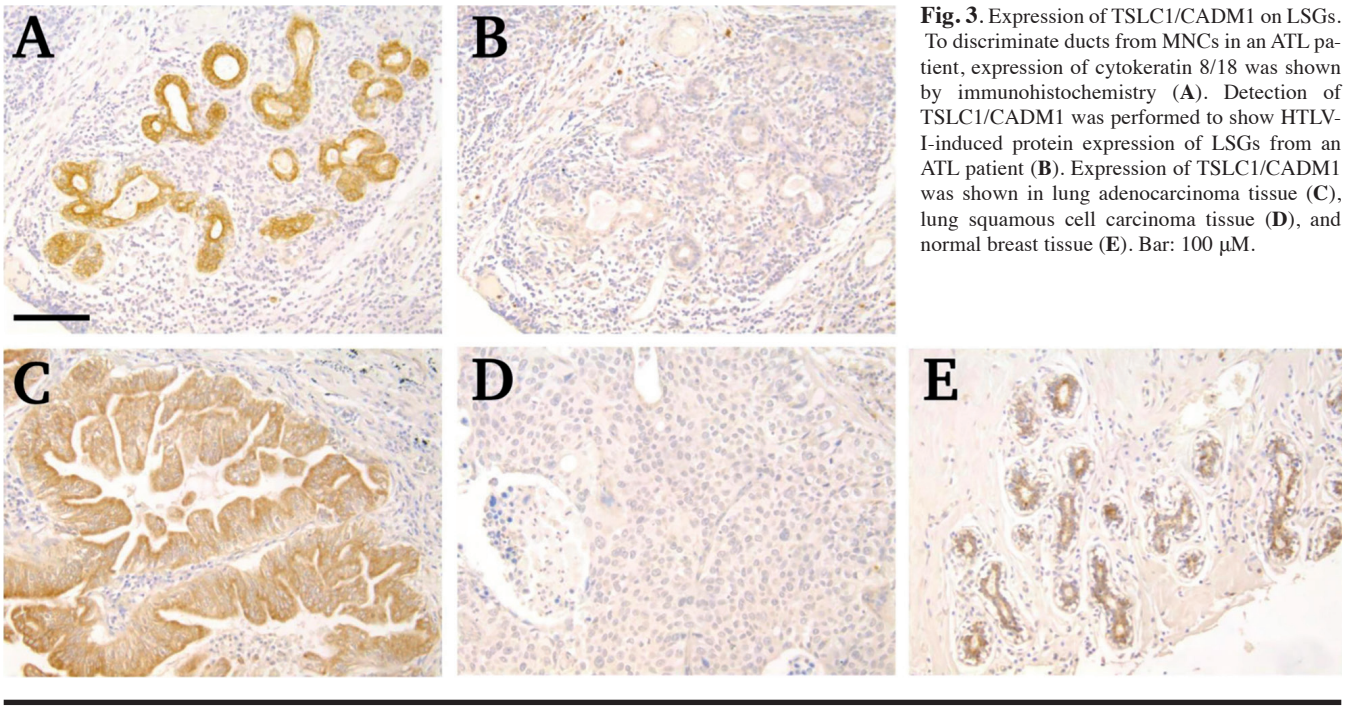

Fig. 3. Expression of TSLC1/CADM1 on LSGs. To discriminate ducts from MNCs in an ATL patient, expression of cytokeratin 8/18 was shown by immunohistochemistry (**A**). Detection of TSLC1/CADM1 was performed to show HTLV-I-induced protein expression of LSGs from an ATL patient (**B**). Expression of TSLC1/CADM1 was shown in lung adenocarcinoma tissue (**C**), lung squamous cell carcinoma tissue (**D**), and normal breast tissue (**E**). Bar: 100 μM.

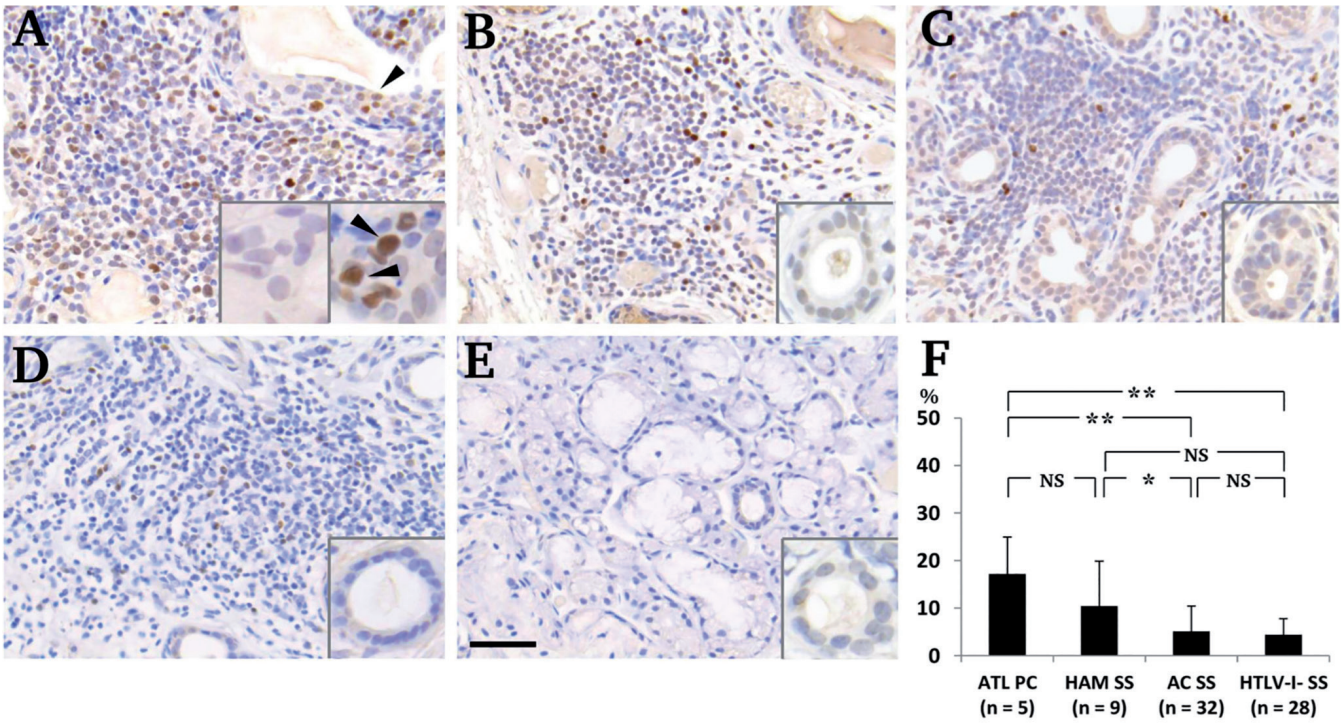

Fig. 4. Expression of Foxp3 in the LSGs of SS patients.
Immunohistochemistry to detect Foxp3 protein expression was performed. LSGs from a patient with ATL (**A**), a HAM-SS patient (**B**), an HTLV-I AC patient with SS (**C**), an HTLV-I-seronegative SS patient (**D**), and a normal control (**E**) were reacted with anti-mouse Foxp3 monoclonal antibody. After incubation with Histofine Simple Stain MAX-PO (M), the brown colour was developed with DAB. Insets show representative ductal expression of Foxp3. The left inset in panel A shows an isotype control, IgG1. Arrowheads in panel A indicate ductal expression of Foxp3. The figures show representative staining pattern from patients in each group. Bar: 40 μM. F: The frequency of the DAB-positive area in each focus was quantitated by using a microcell count system. The number on the longitudinal axis represents the percentage (%) of DAB-positive area. The numbers in parentheses are the numbers of foci, not patients. *p<0.05, **p<0.01 by Student's t-test; PC: positive control; NS: not significant; error bars; standard deviation.

of the *tax* gene and its downstream pro-inflammatory molecules in the MNCs-mediated production of these molecules has been debated (10, 11). In contrast, $CD4^+CD25^+Foxp3^+$Tregs cells are known to have suppressive functions (23), including down-regulation of CD80 mRNA on antigen presenting cells (APCs) and production of anti-inflammatory cytokines (24). In many autoimmune diseases, the ratio of $CD4^+CD25^+Foxp3^+$Tregs cells is

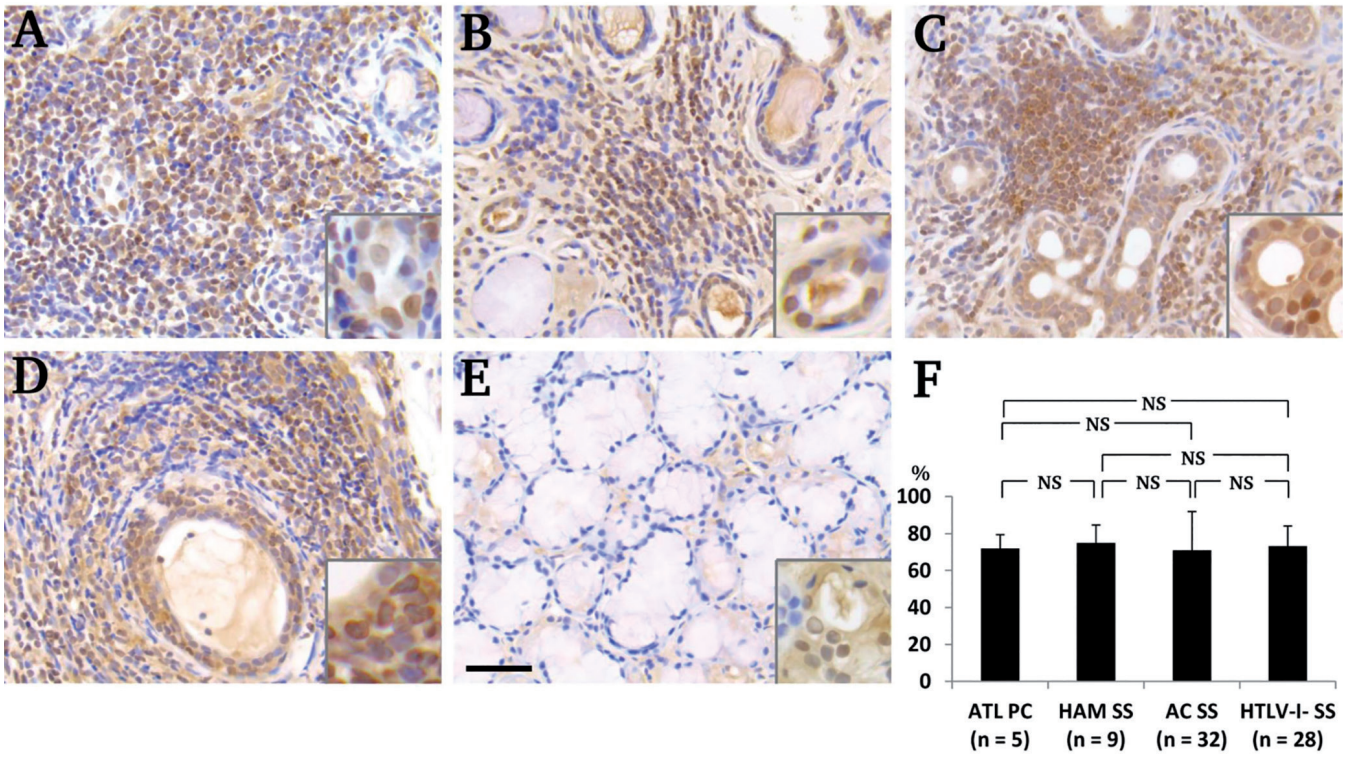

Fig. 5. Expression of p65 in the LSGs of SS patients. Immunohistochemistry to detect NF-κB p65 protein expression was performed. LSGs from a patient with ATL (**A**), a HAM-SS patient (**B**), an HTLV-I AC patient with SS (**C**), an HTLV-I-seronegative SS patient (**D**), and a normal control (**E**) were reacted with anti-rabbit NF-κB p65 polyclonal antibody. After incubation with Histofine Simple Stain MAX-PO (R), the brown colour was developed with DAB. Insets show representative ductal expressions of p65. The figures show representative staining patterns from patients in each group. Bar: 40 μM. F: The frequency of DAB-positive area in each focus was quantitated using a microcell count system. The number on the longitudinal axis represents the percentage (%) of DAB-positive area. The numbers in parentheses are the numbers of foci, not patients. *p<0.05, **p<0.01 by Student's t-test; PC: positive control; NS: not significant; error bars; standard deviation.

known to be associated with the level of inflammation. In contrast, the inflammation detected in ATL has been explained by Foxp3$^+$Tregs cells induced by *HBZ*. Satou *et al*. (25) demonstrated that *HBZ*-transgenic (Tg) mice that develop T-cell lymphoma showed unique characteristics regarding CD4$^+$T cells. Although *HBZ*-Tg mice showed that *HBZ* itself directly increased CD4$^+$Foxp3$^+$T cells, the suppressive function of the proliferated Foxp3$^+$Treg was rather impaired. This paradoxical dysfunction of Foxp3$^+$Tregs regardless of *HBZ*-mediated proliferation of Foxp3$^+$Tregs might have contributed to the inflammation detected in the LSGs from our patient with ATL.

Saito *et al*. (26) reported that HTLV-I AC patients and patients with HAM had high percentages of Foxp3$^+$CD4$^+$T cells in peripheral blood mononuclear cells (PBMCs) compared to those from HTLV-I uninfected individuals. However, differences in the presence of HTLV-I-related genes and Foxp3 in LSGs in SS patients had not been reported before the present study. Although there are conflicting reports (27-29) regarding the number of Foxp3$^+$ regulatory T cells in LSGs of SS patients, our quantitative data suggest that the ATL patient had an *HBZ*-associated increase of Foxp3, although a mechanism of increased Foxp3 in HAM-SS patients is not concluded by the results in this study.

Regarding the specificity of the ISH system, the specificity of the ViewRNA probe was much higher than that of traditional RNA probes, which has already been reported (30) by using a ViewRNA ISH system. Although faint *HBZ* signals were also detected in LSGs from HTLV-I-seronegative subjects and normal subjects, the involvement of *HBZ* and the significance of *HBZ* expression in HTLV-I-seronegative subjects remain to be clarified. However, these might be non-specific signals, since no expression of Foxp3 that should be induced by *HBZ* was detected in the LSGs from normal subjects.

Although it is known that *tax* expression is not observed in PBMCs of all ATL cases (31, 32), the strong positive expression of p65 in our ATL case might have been caused by various pro-inflammatory cytokines produced in ATL cells. Conversely, a mechanism of frequent co-expression of p65 and Foxp3 in MNCs in HAM-SS patients might be different from an ATL because *tax*-mediated NF-κB activation-induced secondary inflammation process or paracrine action toward adjacent lymphocytes is assumable. In addition, the NF-κB pathway is activated by various stimuli (33, 34), thereby, the similar expression pattern of p65 in all patients with SS observed in the present study would not be explained by transactivation of the NF-κB pathway due to HTLV-I infection. In contrast, the different expression patterns of Foxp3 in LSGs are characteristics in this study aside from a direct influ-

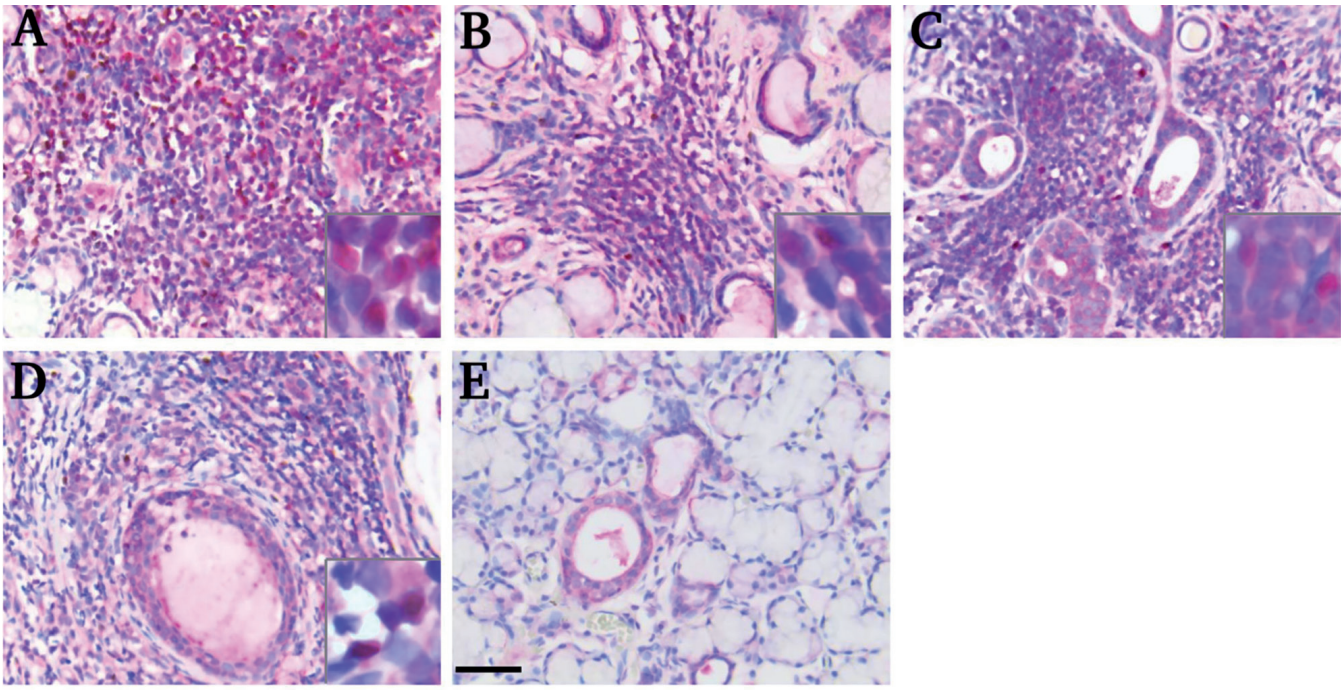

Fig. 6. Co-expression of p65 and Foxp3 in the LSGs of SS patients. Immunohistochemistry against p65 and Foxp3 protein was performed by double staining. LSGs from a patient with ATL (**A**), a HAM-SS patient (**B**), an HTLV-I AC patient with SS (**C**), an HTLV-I-seronegative SS patient (**D**), and a normal control (**E**) were reacted with a mixture of mouse anti-human Foxp3 monoclonal antibody and rabbit anti-human NF-κB p65 polyclonal antibody. After incubation with a mixture of Histofine Simple Stain MAX-PO (M) and AP (R), brown and red colours were developed with DAB and Fast red, respectively. Insets show representative double expression of Foxp3 and p65. The figures show representative staining patterns from patients in each group. Bar: 40 μM.

ence of *HBZ* toward Foxp3 expression. These novel findings detected in LSGs have the potential to be used for discriminating HTLV-I-seropositive SS from HTLV-I-seronegative SS.

Another crucial point is the expression of HTLV-I genes in ductal epithelial cells in LSGs from HTLV-I-seropositive SS patients. HTLV-I has the potential to infect $CD4^+$T cells (35). Two major theories have been proposed regarding the route of HTLV-I infection of uninfected $CD4^+$T cells – namely, the infection could occur via a biofilm-like structure containing HTLV-I viral assemblies (36) or via virological synapses (37). In contrast, we recently observed that HTLV-I has the potential to infect cultured salivary gland epithelial cells (SGECs) and to result in the induction of chemokines and pro-inflammatory cytokines (38). With respect to the *in vitro* infection of HTLV-I, other studies have shown that HTLV-I had the potential to infect epithelial cells other than SGECs or synovial cells (39, 40).

Thus far, HTLV-I infection of salivary gland tissue has not been well investigated, although some studies (41, 42) have reported that HTLV-I-related molecules were expressed in LSGs from SS patients irrespective of HTLV-I infection. Other investigations (43, 44) revealed that *tax* was rarely detected in LSGs from HTLV-I-seronegative patients with SS. *HBZ* in ducts in LSGs from HTLV-I-seropositive SS patients had not been reported prior to the present study. Further studies will be needed to address the question of why the protein expression of Foxp3 is scarce on ducts from ATL and HAM-SS patients irrespective of the frequent ductal *HBZ* expression. Although *HBZ* expression was prominent in ducts from an ATL patient, expression of an ATL surface marker CADM1/ TSLC1 was not detected in Figure 3. As shown in lung adenocarcinoma or normal breast tissue, detection of CADM1/TSLC1 expression was known in carcinoma or normal tissue (45). In peripheral blood of acute ATL patients, the percentage of $CD4^+CADM1^+$ cells were more than 70%. In contrast, the frequency of $CD4^+CADM1^+$ cells in chronic ATL or HTLV-I AC was less than 5% (46). Although the negative CADM1/TSLC1 expression with positive *HBZ* signal was detected in ducts and MNCs from the ATL case in this study, the negative CADM1/TSLC1 expression might depend on clinical entities of ATL as reported previously (46).

There were some limitations of the present study in regard to the comparisons of the *HBZ*/*tax* mRNA level, because the *tax* signal is detected in HAM-SS samples regardless of the reported high *HBZ*/*tax* mRNA ratio (25). First, there is a possibility that the mRNA level varies according to PVL, because *HBZ* mRNA was correlated with PVL in HAM-SS patients. Second, the different nucleotide sequences and sequence lengths of each probe could have had an impact on the visualised signal.

Taken together, our findings indicate that *HBZ* was dominantly expressed in the LSGs of HTLV-I-seropositive SS patients, although MNCs from HAM-SS patients showed *tax*-dominant expression. In addition, the ductal expression of *HBZ* and *tax* may be a newly identified feature of focal inflammation in HTLV-I-infected salivary glands. Regarding HBZ detection at the protein level, two reports have examined lab-generated antibodies against

HBZ (47, 48). With a useful antibody and in vivo detection system in hand, we should be able to detect the HBZ protein in a future study. Hitherto, *tax*-mediated chronic inflammation could presumably be considered a step in the pathogenesis of HTLV-I-seropositive SS. Our new findings suggest the role of an *HBZ*-related inflammatory pathway in the pathological condition of HTLV-I-seropositive SS. The detection of an *HBZ*-related pathway and the involvement of ducts impacts on the underlying mechanism of the linkage between HTLV-I infection and SS.

References

1. MARIETTE X, AGBALIKA F, DANIEL MT *et al*.: Detection of human T lymphotropic virus type I tax gene in salivary gland epithelium from two patients with Sjögren's syndrome. *Arthritis Rheum* 1993; 36: 1423-8.
2. KOMPOLITI A, GAGE B, SHARMA L, DANIELS JC: Human T-cell lymphotropic virus type 1-associated myelopathy, Sjögren's syndrome, and lymphocytic pneumonitis. *Arch Neurol* 1996; 53: 940-2.
3. NAKAMURA H, KAWAKAMI A: What is the evidence for Sjögren's syndrome being triggered by viral infection? Subplot: infections that cause clinical features of Sjögren's syndrome. *Curr Opin Rheumatol* 2016; 28: 390-7.
4. BARONE F, COLAFRANCESCO S: Sjögren's syndrome: from pathogenesis to novel therapeutic targets. *Clin Exp Rheumatol* 2016; 34 (Suppl. 98): S58-62.
5. NAKAMURA H, EGUCHI K, NAKAMURA T *et al*.: High prevalence of Sjögren's syndrome in patients with HTLV-I associated myelopathy. *Ann Rheum Dis* 1997; 56: 167-72.
6. NAKAMURA H, TAKAGI Y, KAWAKAMI A *et al*.: HTLV-I infection results in resistance toward salivary gland destruction of Sjögren's syndrome. *Clin Exp Rheumatol* 2008; 26: 653-5.
7. NAKAMURA H, KAWAKAMI A, HAYASHI T *et al*.: Low prevalence of ectopic germinal centre formation in patients with HTLV-I-associated Sjögren's syndrome. *Rheumatology* (Oxford) 2009; 48: 854-5.
8. IZUMI M, NAKAMURA H, NAKAMURA T, EGUCHI K, NAKAMURA T: Sjögren's syndrome (SS) in patients with human T cell leukemia virus I associated myelopathy: paradoxical features of the major salivary glands compared to classical SS. *J Rheumatol* 1999; 26: 2609-14.
9. NAKAMURA H, SHIMIZU T, TAKAGI Y *et al*.: Reevaluation for clinical manifestations of HTLV-I-seropositive patients with Sjögren's syndrome. *BMC Musculoskelet Disord* 2015; 16: 335.
10. SUMIDA T, YONAHA F, MAEDA T *et al*.: Expression of sequences homologous to HTLV-I tax gene in the labial salivary glands of Japanese patients with Sjögren's syndrome. *Arthritis Rheum* 1994; 37: 545-50.
11. MARIETTE X, AGBALIKA F, ZUCKER-FRANKLIN D *et al*.: Detection of the tax gene of HTLV-I in labial salivary glands from patients with Sjögren's syndrome and other diseases of the oral cavity. *Clin Exp Rheumatol* 2000; 18: 341-7.
12. SHATTLES WG, BROOKES SM, VENABLES PJ, CLARK DA, MAINI RN: Expression of antigen reactive with a monoclonal antibody to HTLV-1 P19 in salivary glands in Sjögren's syndrome. *Clin Exp Immunol* 1992; 89: 46-51.
13. GREEN JE, HINRICHS SH, VOGEL J, JAY D: Exocrinopathy resembling Sjögren's syndrome in HTLV-1 tax transgenic mice. *Nature* 1989; 341: 72-4.
14. ENOSE-AKAHATA Y, ABRAMS A, MASSOUD R *et al*.: Humoral immune response to HTLV-1 basic leucine zipper factor (HBZ) in HTLV-1-infected individuals. *Retrovirology* 2013; 10: 19.
15. YAMAMOTO-TAGUCHI N, SATOU Y, MIYAZATO P *et al*.: HTLV-1 bZIP factor induces inflammation through labile Foxp3 expression. *PLoS Pathog* 2013; 9: e1003630.
16. MATSUBAR Y, HORI T, MORITA R, SAKAGUCHI S, UCHIYAMA T: Delineation of immunoregulatory properties of adult T-cell leukemia cells. *Int J Hematol* 2006; 84: 63-9.
17. VITALI C, BOMBARDIERI S, JONSSON R *et al*.: Classification criteria for Sjögren's syndrome: a revised Version of the European criteria proposed by the American-European Consensus Group. *Ann Rheum Dis* 2002; 61: 554-8.
18. OHTA M, OHTA K, NISHIMURA M, SAIDA T: Detection of myelin basic protein in cerebrospinal fluid and serum from patients with HTLV-1-associated myelopathy/tropical spastic paraparesis. *Ann Clin Biochem* 2002; 39: 603-5.
19. NAKAMURA H, IWAMOTO N, HORAI Y *et al*.: A case of adult T-cell leukemia presenting primary Sjögren's syndrome-like symptoms. *Int J Rheum Dis* 2013; 16: 489-92.
20. FUJIMOTO T, HATA T, ITOYAMA T *et al*.: High rate of chromosomal abnormalities in HTLV-I-infected T-cell colonies derived from prodromal phase of adult T-cell leukemia: a study of IL-2-stimulated colony formation in methylcellulose. *Cancer Genet Cytogenet* 1999; 109: 1-13.
21. OHYAMA Y, NAKAMURA S, HARA H *et al*.: Accumulation of human T lymphotropic virus type I-infected T cells in the salivary glands of patients with human T lymphotropic virus type I-associated Sjögren's syndrome. *Arthritis Rheum* 1998; 41: 1972-8.
22. ZHAO LJ, GIAM CZ: Human T-cell lymphotropic virus type I (HTLV-I) transcriptional activator, Tax, enhances CREB binding to HTLV-I 21-base-pair repeats by protein-protein interaction. *Proc Natl Acad Sci USA* 1992; 89: 7070-4.
23. SAKAGUCHI S, YAMAGUCHI T, NOMURA T, ONO M: Regulatory T cells and immune tolerance. *Cell* 2008; 133: 775-87.
24. GRANT CR, LIBERAL R, MIELI-VERGANI G, VERGANI D, LONGHI MS: Regulatory T-cells in autoimmune diseases: challenges, controversies and--yet--unanswered questions. *Autoimmun Rev* 2015; 14: 105-16.
25. SATOU Y, YASUNAGA J, ZHAO T *et al*.: HTLV-1 bZIP factor induces T-cell lymphoma and systemic inflammation *in vivo*. *PLoS Pathog* 2011; 7: e1001274.
26. SAITO M, MATSUZAKI T, SATOU Y *et al*.: *In vivo* expression of the HBZ gene of HTLV-1 correlates with proviral load, inflammatory markers and disease severity in HTLV-1 associated myelopathy/tropical spastic paraparesis (HAM/TSP). *Retrovirology* 2009; 6: 19.
27. SARIGUL M, YAZISIZ V, BASSORGUN CI *et al*.: The numbers of Foxp3 + Treg cells are positively correlated with higher grade of infiltration at the salivary glands in primary Sjögren's syndrome. *Lupus* 2010; 19: 138-45.
28. BANICA L, BESLIU A, PISTOL G *et al*.: Quantification and molecular characterization of regulatory T cells in connective tissue diseases. *Autoimmunity* 2009; 42: 41-9.
29. LI X, LI X, QIAN L *et al*.: T regulatory cells are markedly diminished in diseased salivary glands of patients with primary Sjögren's syndrome. *J Rheumatol* 2007; 34: 2438-45.
30. DUONG FH, TRINCUCCI G, BOLDANOVA T *et al*.: IFN-λ receptor 1 expression is induced in chronic hepatitis C and correlates with the IFN-λ3 genotype and with nonresponsiveness to IFN-α therapies. *J Exp Med* 2014; 211: 857-68.
31. GIAM CZ, JEANG KT: HTLV-1 Tax and adult T-cell leukemia. *Front Biosci* 2007; 12: 1496-507.
32. JEANG KT: Functional activities of the human T-cell leukemia virus type I Tax oncoprotein: cellular signaling through NF-kappa B. *Cytokine Growth Factor Rev* 2001; 12: 207-17.
33. OBATA H, BIRO S, ARIMA N *et al*.: NF-kappa B is induced in the nuclei of cultured rat aortic smooth muscle cells by stimulation of various growth factors. *Biochem Biophys Res Commun* 1996; 224: 27-32.
34. NISHI Y, TAKENO S, ISHINO T, HIRAKAWA K: Glucocorticoids suppress NF-kappaB activation induced by LPS and PGN in paranasal sinus epithelial cells. *Rhinology* 2009; 47: 413-8.
35. GOON PK, IGAKURA T, HANON E *et al*.: Human T cell lymphotropic virus type I (HTLV-I)-specific $CD4^+$ T cells: immunodominance hierarchy and preferential infection with HTLV-I. *J Immunol* 2004; 172: 1735-43.
36. PAIS-CORREIA AM, SACHSE M, GUADAGNINI S *et al*.: Biofilm-like extracellular viral assemblies mediate HTLV-1 cell-to-cell transmission at virological synapses. *Nat Med* 2010; 16: 83-9.
37. IGAKURA T, STINCHCOMBE JC, GOON PK *et al*.: Spread of HTLV-I between lymphocytes by virus-induced polarization of the cytoskeleton. *Science* 2003; 299: 1713-6.
38. NAKAMURA H, TAKAHASHI Y, YAMAMOTO-FUKUDA T *et al*.: Direct infection of primary salivary gland epithelial cells by human T lymphotropic virus type I in patients with Sjögren's syndrome. *Arthritis Rheumatol* 2015; 67: 1096-106.
39. LIU B, LI Z, MAHESH SP, KURUP SK, GIAM CZ, NUSSENBLATT RB: HTLV-1 infection of human retinal pigment epithelial cells and inhibition of viral infection by an antibody

to ICAM-1. *Invest Ophthalmol Vis Sci* 2006; 47: 1510-5.

40. SAKAI M, EGUCHI K, TERADA K *et al*.: Infection of human synovial cells by human T cell lymphotropic virus type I. Proliferation and granulocyte/macrophage colony-stimulating factor production by synovial cells. *J Clin Invest* 1993; 92: 1957-66.
41. LEE SJ, LEE JS, SHIN MG *et al*.: Detection of HTLV-1 in the labial salivary glands of patients with Sjögren's syndrome: a distinct clinical subgroup? *J Rheumatol* 2012; 39: 809-15.
42. TALAL N, DAUPHINÉE MJ, DANG H, ALEXANDER SS, HART DJ, GARRY RF: Detection of serum antibodies to retroviral proteins in patients with primary Sjögren's syndrome (autoimmune exocrinopathy). *Arthritis Rheum* 1990; 33: 774-81.
43. MIZOKAMI A, EGUCHI K, MORIUCHI R *et al*.: Low copy numbers of human T-cell lymphotropic virus type I (HTLV-I) tax-like DNA detected in the salivary gland of seronegative patients with Sjögren's syndrome in an HTLV-I endemic area. *Scand J Rheumatol* 1998; 27: 435-40.
44. RIGBY SP, COOKE SP, WEERASINGHE D, VENABLES PJ: Absence of HTLV-1 tax in Sjögren's syndrome. *Arthritis Rheum* 1996; 39: 1609-11.
45. ZENG D, WU X, ZHENG J *et al*.: Loss of CADM1/TSLC1 expression is associated with poor clinical outcome in patients with esophageal squamous cell carcinoma. *Gastroenterol Res Pract* 2016; 2016: 6947623.
46. NAKAHATA S, MORISHITA K: CADM1/TSLC1 is a novel cell surface marker for adult T-cell leukemia/lymphoma. *J Clin Exp Hematop* 2012; 52: 17-22.
47. RAVAL GU, BIDOIA C, FORLANI G, TOSI G, GESSAIN A, ACCOLLA RS: Localization, quantification and interaction with host factors of endogenous HTLV-1 HBZ protein in infected cells and ATL. *Retrovirology* 2015; 12: 59.
48. SHIOHAMA Y, NAITO T, MATSUZAKI T *et al*.: Absolute quantification of HTLV-1 basic leucine zipper factor (HBZ) protein and its plasma antibody in HTLV-1 infected individuals with different clinical status. *Retrovirology* 2016; 13: 29.